Study of InP(100)nitridation using AES spectroscopy and electrical analysis: Effect of annealing after nitridation.

A. TALBI[a*], M. A. BENAMARA[a], M. TALBI[b], Z. BENAMARA[a], B. AKKAL[a], B. GRUZZA[c], C. ROBERT-GOUMET[c], L. BIDEUX[c], G. MONIER[c]

[a]*Laboratoire de Microélectronique Appliquée Université Djillali LIABÈS de Sidi Bel Abbés 22000, Algérie.*

[b]*Faculté de Médecine. Université Djillali LIABES de Sidi Bel Abbés 22000, Algérie.*

[c]*LAboratoire des Sciences des Matériaux pour l'Electronique et d'Automatique, Université Blaise Pascal de Clermont II, Les Cézeaux, 63177, Aubière Cedex, France.*

Auger electron spectroscopy (AES) was used to understand the different steps of the indium phosphide nitridation and the annealing of the InN films. The AES analysis combined with electrical characterisation using the current-voltage I(V). After ionic cleaning with Ar^+ ions, metallic indium crystallites are created and the nitridation of the InP substrates is performed using a plasma Glow discharge source (GDS). We used the In_{MNN}, N_{KLL} and P_{LMM} Auger transitions to monitor the chemical state of the surface. We observed that after nitridation, the creation of InN and P-N bonds while the In-In metallic bonds decrease. This confirms the reaction between indium clusters and nitrogen species. After these operations, we observed the effect of annealing on the nitridated layers at 450 °C during 15 min. It appears after heating that the In-N bonds decreases and the P-N bonds increases. A theoretical model based on stacked layers allows us to confirm that two monolayers of indium nitride are created on InP (100) surface. After this operation we note a presence of an important quantity of metallic indium at the surface using Auger analysis. In fact, the (I-V) characteristics reveal a low series resistance (168Ω) for the annealed sample compared with a value of 1687Ω obtained in the not annealed ones. We believe it's caused by the destruction of the nitride layer. The results obtained with AES spectra are coherent with electrical measurements; they suggest that the InN films are significantly affected by the temperature.

(Received April 17, 2013; accepted June 12, 2013)

Keywords: Nitridation, AES, Indium phosphide (100), Electrical properties, Barrier height, Annealing

1. Introduction

The nitridated compounds are currently the most promising semiconductors for opto-and microelectronics application. During the last few years, the interest in the indium nitride (InN) semiconductor has been remarkable and the number of papers concerning InN has significantly increased [1, 2].

The InP surfaces nitridation has different interests as the realisation of InN buffer layers before the InN films growth, or as passivated layers. Different methods have been investigated for the nitridation of InP(100) surfaces[3, 4].In our study, we have used the plasma nitridation method [5].

It is known that the nitrogen parameters influence the structural and electronic properties of the nitridated surfaces. In this paper, thin InN film is realised by the nitridation of InP substrates using a Glow Discharge Source (GDS). This nitridation process is monitored by Auger Electron Spectroscopy (AES) and electrical characterisation in the aim to analyze the evolution of the surface and to determine the electrical properties of InN/InP interface. We also report in this paper the effect of annealing (T=450 °C, t= 15 min) [6, 7] on the nitridated samples. A theoretical model has been elaborated to interpret the experimental results.

2. Experimental procedures

S-Doped InP (100) wafers have been used with carrier concentration of 10^{15} cm^{-3}; they were chemically cleaned in different ultrasonic baths [8] (H_2SO_4, 3% bromine methanol deionised water). After introduction into the ultra high vacuum chamber (10^{-7} Pa), a low amount of carbon and oxygen contaminations was detected. These impurities were removed by in situ cleaning with low energy Ar^+ ions (ion energy 300 eV; sample current 2μA/cm^2, t=15min) [9]. The ionic bombardment is a key step in the nitridation process since it creates at the surface metallic indium in well-controlled quantities

(mean coverage: 25%, mean height: 4 atomic monolayers) by preferential phosphorus sputtering [10]. This is equivalent to one complete atomic monolayer In-In. Therefore, the maximum number of indium nitride layers which can be formed by the consumption of the indium droplets by nitrogen is two monolayers.

The nitridation process has been performed with a high voltage plasma discharge cell. In this kind of nitrogen source, a high voltage (about 2 kV) produces continuous plasma. A majority of N atomic species are created. The samples are heated at 250°C during the nitridation process, according to previous work investigating the influence of the temperature on the nitridation process [11-9].

The indium droplets layers are consumed by nitrogen atomic species. During the nitridation process, the samples were kept under a grazing nitrogen flow during 40min. A Nitrogen flow inside the chamber was equal to 10^{-1} Pa. After the nitridation the samples are heated in situ at 450 °C for 15 min. The different in situ steps are monitored by Auger spectroscopy. A model based on stacked layers has been used to interpret the AES results.

The electrical parameters of the InN/InP structures before and after annealing are also determined using I(V)measurements, these characterizations are performed using HP 4155 (semiconductor parameter analyser). The InN/InP structures are tested with a mercury probe used as a temporary gate contact.

3. Results and discussion

3.1. Auger analysis

The nitridation of InP (100) substrates was investigated using AES analysis. The measurements have been carried out simultaneously with the nitridation process and annealing. We have recorded during experiments the Auger signal of In_{MNN} (E=403 and 411eV), of N_{KLL} (E=383eV) and of P_{LMM} (E=117eV).

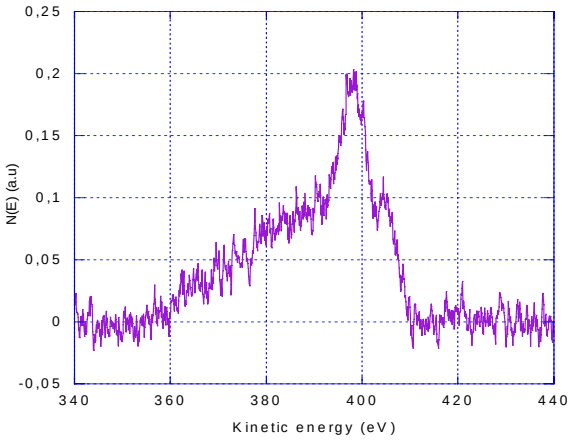

Fig. 1. Indium Auger transition after ionic cleaning.

Fig.1 shows the evolution of the In_{MNN} Auger peak after ionic cleaning. Previous works [10, 12] showed that after ionic cleaning, the surface is covered by 25% of metallic indium droplets with an equivalent height of 4 monolayers. Indium droplets are created by preferential phosphorus sputtering.

The evolution of $In_{MNN,}$ N_{KLL} Auger transitions after the nitridation process is presented in Fig.2. The transition N_{KLL} (E=383eV) appears after the nitridation, confirming the presence of nitrogen on the surface, the apparition of this peak is accompanied simultaneously with an attenuation of the indium signal, we have calculate, $R_{exp\ In}$ the ratio between the indium signal intensity after nitridation and the indium signal intensity after cleaning, this one is about 0.87. The indium droplets created by the ion bombardment cleaning are consumed by nitrogen species coming from a glow discharge source (GDS) to create nitride layers.

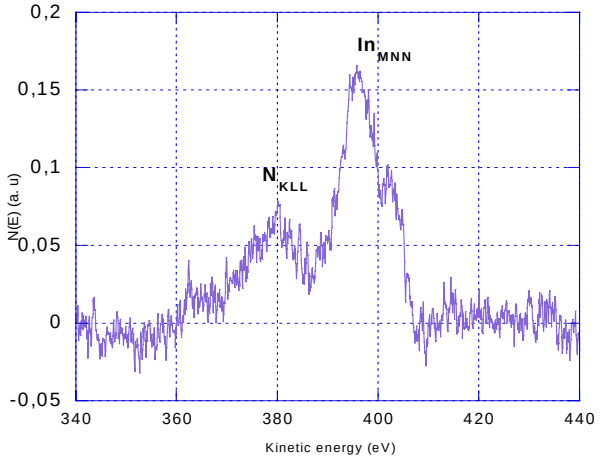

Fig. 2. Indium and nitrogen Auger transition before annealing.

The evolution of the In Auger peak after annealing is displayed in Fig.3, we observe that the indium intensity increase, we notice that the value of the $R_{exp\ In}$ the ratio between the indium peak intensity after annealing and the indium peak intensity after nitridation is superior to 1. On the contrary, for nitrogen the Auger signal intensity decreases, it's probably due to a destruction of nitride layers.

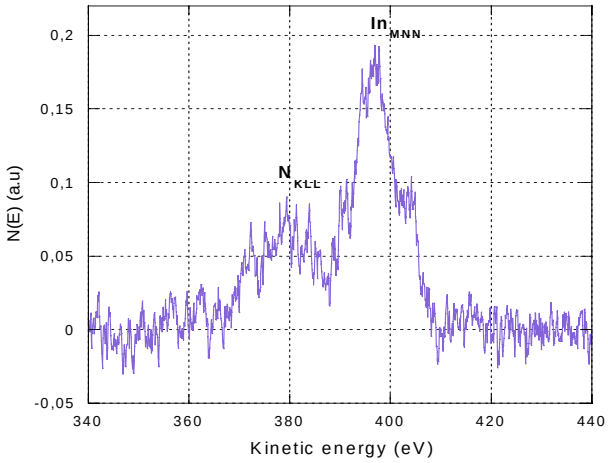

Fig. 3. Indium and nitrogen Auger transition after annealing.

The evolution of the Auger spectrum of phosphorus (P_{LMM}) after different steps is presented in Figs(4, 5, and 6). After Ar^+ cleaning, this peak can be decomposed into three Gaussians, being characteristic of the three groups of transitions. The first component, (A_{exp}) is characteristic of the sum of the $L_3M_1M_1$ and $L_2M_1M_1$ Auger transitions of phosphorus; these two transitions are very close to each other and can be represented by only one peak at 97 eV. The second peak, (B_{exp}), is the sum of the $L_3M_1M_{23}$ and $L_2M_1M_{23}$ Auger transitions of phosphorus; it is located at the energy of 106 eV. Finally the last peak,(C_{exp}), is

characteristic of the sum of the $L_3M_{23}M_{23}$ and $L_2M_{23}M_{23}$ Auger transitions of phosphorus at 116 eV. Table 1 presents the comparison of the experimental peak energies and heights with the calculated ones [13], named A_{th}, B_{th}, and C_{th},[14].

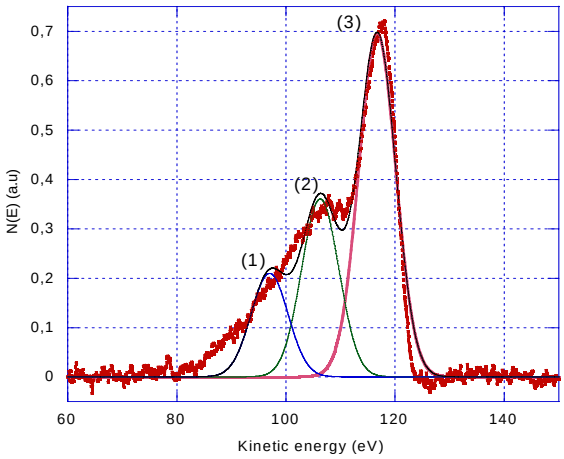

Fig. 4. Phosphorus Auger transition after ionic bombardment.

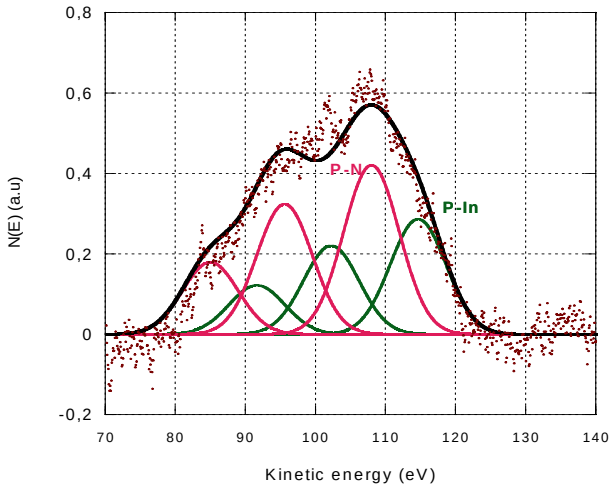

Fig. 5. Phosphorus Auger pic decomposition before annealing.

After nitridation, we noticed a change in the phosphorus peak shape, which is related to the presence of P-N bonds. This peak cannot be decomposed into three gaussians; a new group of transitions has appeared. We found an energy shift of 8 eV between the two groups of transitions. This shift can be explained by the P-N bonds or charge transfer at the surface of the substrate. Therefore, the experimental peak can be decomposed into three pairs of Gaussians. Parameters were conserved: the ratio of the heights, the shift in energy and the full width at half maximum (FWHM). We can define $R_{expP\text{-}In}$ as the ratio between the sum of the areas of P-In gaussians and the total area of the phosphorus peak. $R_{expP\text{-}N}$ is the area ratio between the sum of the areas of P-N gaussians and the total area of the phosphorus peak. These values are about 0.404 and 0.595 respectively. We can observe that after nitridation, $R_{expP\text{-}N}$ is superior to $R_{expP\text{-}In}$. After annealing, $R_{exp\ P\text{-}In}$ decreases it's equal to 0.354 and $R_{exp\ P\text{-}N}$ increases it's about 0.6458. The quantity of P-N bonds is so higher than the P-In bonds (see Fig. 6). This phenomenon is attributed to the damaging of the InN layer and to rupture of the P-In bonds. Consequently the nitrogen diffuses into the interface InN/InP and forms other P-N bonds with the phosphorus.

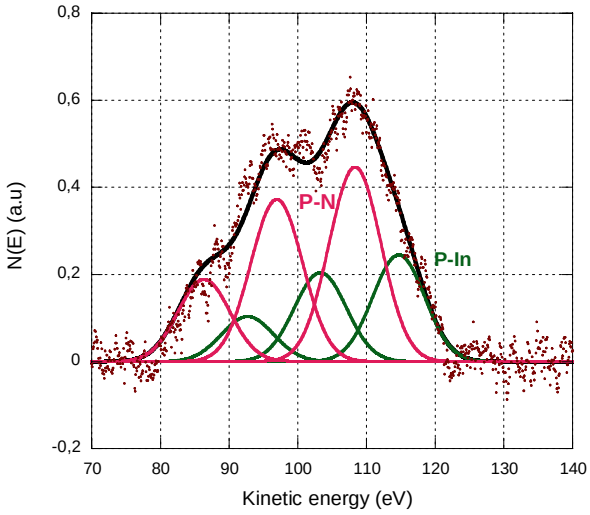

Fig. 6. Phosphorus Auger pic decomposition after annealing.

3.2 Theoretical model

To interpret the AES experimental results a theoretical model based on stacked layers has been used. Moreover for each signal, we can calculate the theoretical intensity as follows [2,7]:

The total intensity of indium AES signal is:

$$I_{indium} = 0.25\,(1 + \alpha_{In} + \alpha_{In}^2 + \alpha_{In}^3)\,i_{In} + (0.75 + 0.25\,\alpha_{In}^4)\,\frac{\alpha_{In}.i_{In}}{1-\alpha_{In}^2} \quad (1)$$

with:

i_{In}: is the intensity of one atomic monolayer of indium;

α_{In}: the attenuation coefficient of the indium Auger current through a P or In atomic monolayer, it is given by:

$$\alpha_{In} = \exp\left(-\frac{d}{0.85\,\lambda_{i_{In}}}\right)$$

$\lambda_{i_{In}}$: is the mean free path of Auger electrons [15];

d : is the thickness layer.

Then the numerical value of α_{In} is equal to 0.73.

After the nitridation all indium crystallites were consumed, so we can consider that the coverage rate of the

surface by the nitride layers was equal to unity and that there were two monolayers of indium nitride [2, 7].

The theoretical ratio $I_{In\ after\ nitridation}/I_{In\ after\ bombardment}$ is written:

$$R_{th\,In} = \frac{0.5\left(1+\alpha_{In}\right)+\dfrac{\alpha_{In}^3}{\left(1-\alpha_{In}^2\right)}}{0.25\left(1+\alpha_{In}+\alpha_{In}^2+\alpha_{In}^3\right)+\left(0.75+0.25\alpha_{In}^4\right)\dfrac{\alpha_{In}}{\left(1-\alpha_{In}^2\right)}} \quad (2)$$

The theoretical ratio is equal to R_{thIn}= 0.873 close to the experimental value witch is estimated at 0.89. It confirms that we have formed two monolayers of stoichiometric indium nitride.

Thus, the theoretical intensity of the phosphorus Auger signal after the nitridation is equal to

$$I_P = I_{P-N} + I_{P-In} = \alpha_p^2 . i_p + \left(\alpha_p^4 / \left(1-\alpha_p^2\right)\right) i_p = 0.43\, i_p \quad (3)$$

We defined $R_{thP\text{-}N}$ and $R_{thP\text{-}In}$ as the ratios between the signal intensity coming from P-N and from P-In contribution and the total intensity of phosphorus signal respectively after nitridation.

The values of theoretical ratios $R_{thP\text{-}In}$ and $R_{thP\text{-}N}$ calculated for two monolayers of InN are equal to 0.302 and 0.7 respectively. We observed that $R_{thP\text{-}N}$ is greater than $R_{thP\text{-}In}$. These values are in a good agreement with those obtained experimentally.

3.3 Electrical measurements

We plotted I(V) characteristics of InN/InP samples after nitridation and after annealing operations.

The Fig.7 shows the I-V current voltage characteristics for the samples after nitridation and after annealing. The curve obtained after nitridation shows that the realized interface presents a good rectifier contact.

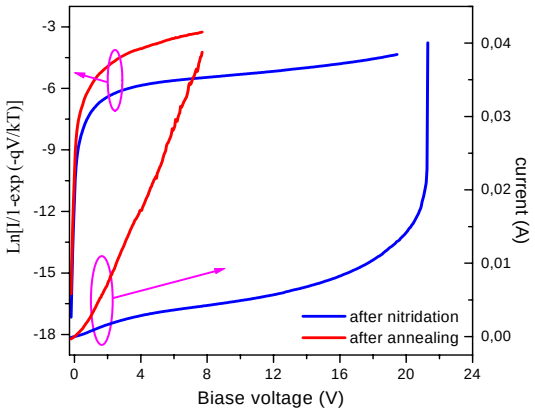

Fig. 7: $\ln\left[I\Big/\left(1-\exp\left(\dfrac{qV}{kT}\right)\right)\right] = f(V)$ *and Current-voltage (I-V) characteristics of the InN/InP structures before and after annealing.*

Owing to fact that the thickness δ of the InN layer is thin, our structures are similar to Schottky diodes. Then the current is expressed as follow: [16, 17]

$$I(V) = I_s\left(\left(1-\exp\left(\frac{-qV}{kT}\right)\right).\exp\left(\frac{qV}{n.kT}\right)\right) \quad (4)$$

where: V is the bias voltage; n is the ideality factor, I_S is the saturation current. The barrier height ϕ_{BN} is related to I_S by

$$\phi_{BN} = \frac{kT}{q}\ln\left(\frac{A^*.T^2}{I_s}\right) \quad (5)$$

where: A^* is the Richardson constant.

The $\ln\left[I\Big/\left(1-\exp\left(\dfrac{qV}{kT}\right)\right)\right] = f(V)$ characteristics present two linear regions separated by a transition segment. As the current is low, the bias voltage may be considered equal to the bias applied to the InP semiconductor depletion layer. The ideality factor n expresses the deviation between ideal and real behaviours [18], its value is equal to 2.98. The saturation current I_s is obtained using the intercept on the current axis of the characteristic given in the Fig. 7 of the first region. Then, the saturation current is estimated to 1.061×10^{-5}A. By substituting the values of I_s in eq. 5,we have deduced the height of the potential barrier ϕ_{BN} which is equal to 0.504 V. This value is comparable with that obtained by M. Petit and al.[19]. When the current becomes somewhat high, the above considerations are not valid, so we must take into account the effect of serial resistance R_s. In Fig. 7when the bias voltage increases, we show clearly the change in the slope of the $\ln\left[I\Big/\left(1-\exp\left(\dfrac{qV}{kT}\right)\right)\right]$ characteristics. Using these approximations and analyzing the region 2, we have estimated the value of the serial resistance R_s to 1687 Ω. The high values of the serial resistance can be attributed to the InN layers, wich are not intentionally doped.

Table .1 Comparison of theoretical and experimental phosphorus Auger transitions.

Group of transitions	ΔE (eV)	Height
(1) Experiment Theory	- 19 - 14	30 44
(2) Experiment Theory	- 9 - 7	52 66
(3) Experiment Theory	0 0	100 100

The similar experiments have been made on InN/InP samples whose are heated after nitridation at (450°C during 15 min). The measured characteristics are presented in Fig. 7. This curve presents different behaviour compared to first samples (before annealing), In fact we have an ohmic contact. The structure corresponds to a resistance of 186 Ω. It's very low compared with the serial resistance obtained after nitridation. This may be explained by the deterioration of the InN layers and the presence of an important quantity of metallic indium at the surface. This result confirms the one observed by the AES analysis. The obtained electrical parameters are reported in Table 2.

Table. 2: Electrical parameters of Hg/InN/InP structures.

Sample	Hg/InN/InP (before annealing)	Hg/InN/InP (after annealing)
I_s (A)	1.061×10^{-5}	3.71×10^{-5}
n	2.98	2.89
ϕ_{BN}(V)	0.504	0.473
R_s(KΩ)	1.687	0.186

4. Conclusion

In this paper, we have studied the nitridation and the effect of annealing after nitridation of indium phosphide surface. The nitridation of InP (100) surface with a GDS cell has been examined in situ using Auger electron spectroscopy.

The experimental ratios are closed to the theoretical ratios calculated by the theoretical model based on stacked layers. The results show that almost two monolayers of stoichiometric indium nitride have been formed on the surface after nitridation.

After annealing at 450°C we observe increasing of indium intensity and decreasing of nitrogen Auger signal intensity, this phenomenon is attributed to the damaging of InN layers and the rupture of P-In bonds.Witch induces the diffusion of nitrogen into the interface InN/InP to form other P-N bonds with the phosphorus present at the interface.

The studied structures are electrically characterised using I-V analysis. The saturation current I_s, the mean ideality factor η, the barrier height ϕ_{BN} and the serial resistance R_s are determined.

The current-voltage characteristics obtained after nitridation shows that the interface realised present a good rectifier contact with high serial resistance R_s of 1687Ω.This value is attributed to the InN layers who is not intentionally doped and to the non homogeneity of the InN films.

The I(V) curves obtained after annealing present an ohmic contact tendency. The Auger study of In and P transitions explained this behaviour. In fact, an important quantity of metallic indium is observed at the surface of the samples. This phenomena is confirmed by the serial resistance who decreases and is equal to 186Ω.

References

[1] S. C. Binari, H. C. Dietrich, in: S.J. Pearton (ED), GaN and Related Materials, Gordon and Breach, New York, 1997, p. 509.

[2] M. Losurdo, P. Capezutto, G. Leo, E.A. Irene, J. Vac. Sci. Technol., A **17**(4), 2194 (1999).

[3] J. S. Pan, A.T.S. Wee, C.H.A. Huan, H.S. Tan, K.L. Tan, J. Phys. D: Appl. Physi. **29**, 2997 (1996).

[4] G. Beuchet, M. Bennet, P. Thebault, J.P. Duchemin, J. Cryst. Growth **54**, 379 (1982).

[5] A. Talbi, Z. Benamara, B. Akkal, B. Gruzza, L. Bideux, C. Robert, C. Varenne, N. Chami Material Science and Engineering A. **437**, 254 (2006).

[6] L. Bideux, Y. Ould-Metidji, B. Gruzza, V. Matolin, Surf. Interface Anal.**34**(1), 712 (2002).

[7] M. Petit, D. Baca, S. Arabasz, L. Bideux, N. Tsud, S. Fabik, B. Gruzza, V. Chab, V. Matolin, K. C. Prince, Surf. Sci. **523**, 205 (2005).

[8] J. D. Hecht, F. Frost, T. Chassé, D. Hirsch, H. Neuman, A. Schindler, F. Bigl, Appl. Surf. Sci. **179**, 196 (2001).

[9] M. Petit, Y. Ould-Metidji, C. Robert, L. Bideux, B. Gruzza, V. Matolin, Appl. Surf. Sci. **212- 213**, 601 (2003).

[10] B. Gruzza, C. Pariset, Surface Science **162**, 202 (1985).

[11] Y. Ould-Metidji, L. Bideux, V. Matolin, B. Gruzza, C. Robert, Vacuum,**63**, 229 (2001).

[12] P.S. Mangat, P. Soukiassian, Y. Huttel, Z. Hurych, B. Gruzza, A. Porte, Appl. Phys. Lett. **63**(14), 1957 (1993).

[13] W. A. Coghlan, R. E. Clausing, A catalog of calculated Auger transitions for the elements. Oak Ridge National Laboratory, ORNL-TM-3576, November 1971.

[14] C. Jardin, D. Robert, B. Achard, B. Gruzza, C. Pariset, Surf. Interface Anal. **10**, 301 (1987)

[15] S. TouggardQuases IMFP-TPP2M: Calculation of inelastic electron mean free path by TPP2M, Ver 2.1. Copyright ©1998-2000.

[16] A. Singh Solid state electronics, **26**, 815 (1983).

[17] S.M. Sze (Ed.), Physics of Semiconductors Devices, Wiley & Sons, New York, 1981.

[18] A. Jelenski, E. Kollberg, M.V. Schanerder, H.Zirath, Prog.15 Europ. Microw. Conf. 279-284 (1985)

[19] M. Petit, Ch. Robert-Goumet, L. Bideux, B. Gruzza, Z. Benamara, N. Bachir Bouiadjra, V. Matolin, Appl. Surf. Sci. **234**, 451 (2004).

*Corresponding author:talbi_a02@yahoo.fr